Journal of Nano- and Electronic Physics
Vol. **12** No 4, 04018(5pp) (2020)

Журнал нано- та електронної фізики
Том **12** № 4, 04018(5cc) (2020)

Sintering Temperature Dependent Structural and Mechanical Studies of $Ba_xPb_{1-x}TiO_3$ Ferroelectrics

Sadiya Kazi[1], Feeda Savanur[1], Sushant Kakati[2], Shridhar N. Mathad[2,*], P.R. Jeergal[1], A.S. Pujar[3], C.S. Hiremath[4], S.L. Galgali[3], M.K. Rendale[5], R.B. Pujar[1]

[1] *Departmant of Physics, P.C. Jabin Science College, Hubballi, India*
[2] *Department of Engineering Physics, K.L.E. Institute of Technology, Gokul Road, Hubballi, 580027 Karnataka, India*
[3] *Department of Physics, KLE's RLS Institute, Belgavi, India*
[4] *Department of Physics, H.S. Kotambri Science Institute, Hubballi, India*
[5] *Department of Physics, Gogte Institute of Technology, Belgavi, India*

(Received 25 March 2020; revised manuscript received 15 August 2020; published online 25 August 2020)

Lead-Barium-Titanate (PBT) ferroelectric ceramic has been synthesized by using solid state reaction technique with different sintering temperatures. Structure of the samples was characterized by X-ray diffraction (XRD), scanning electron microscopy (SEM) and Fourier transform infrared spectroscopy (FTIR). XRD of the Pb-Ba-TiO_3 samples confirms the tetragonal perovskite ferroelectric structure with lattice parameters in the range 3.94-3.987 Å and 4.068-4.22 Å, respectively. The grain growth increases with sintering temperature and the grain size of these samples is observed in the range 0.6-1.713 μm from SEM analysis. The absorption bands around 575 cm^{-1} to 585 cm^{-1} are assigned to the stretching vibrations of Ti–O bonds from FTIR analysis. The crystallite size (D), lattice constant (a), microstrain (ε), and dislocation density (ρ_D) are also reported. The Williamson-Hall plot and size-strain plot are also employed to understand the structural and mechanical attributes of ferroelectric samples. Thus, we report variation of structural and mechanical properties of PBT with respect to sintering temperature.

Keywords: X-ray diffraction, Ferroelectrics, Morphology.

DOI: 10.21272/jnep.12(4).04018 PACS numbers: 61.10.Nz, 77.90. + k, 68.55.Jk

1. INTRODUCTION

The ferroelectric (FE) materials on the basis of barium titanate (BTO) have been well studied and have found wide use in engineering [2]. FE polymers are analyzed comprising initial polling, short-circuiting and polarization as switching materials [3], internal mechanical stresses arising in Si-SiO_2-PZT structures [4]. Polycrystalline BST thin films with thickness ranging from 150 nm to 550 nm were prepared by the RF magnetron sputtering and switchable polarization [5]. Lead-free ferroelectrics have drawn much attention due to worldwide concern over the toxicity of lead-containing materials [6, 7]. In view of environmental concerns, strontium barium niobate (bulk and thick films) and Zr doped barium titanate were synthesized by the solid-state method. Detailed structural, dielectric and microwave properties of these materials were reported in [8-10].

Nanosized barium titanate (BT) is the most important FE ceramic material, in which Ba^{2+} ions occupy a corner, while O^{2-} ions are in the phase center and Ti^{4+} ions occupy the body center in the structure, and which has very good dielectric and thermal properties. It is used in different fields like capacitors, piezoelectric sensors and electro-optical devices [11], gas sensors [12], luminescent materials [13], storage devices [14], etc.

Sintering temperature enhances the dielectric, piezoelectric and FE properties of $BaTiO_3$. Increasing temperature of PBT materials changes their phase (tetragonal to a cubic) transition with temperature.

The temperature dependence of lead substituted dielectric materials was studied and it was found that it is better than pure barium titanate. The composition prepared by solid state reactions, according to XRD data, suggests that the synthesized materials have a tetragonal perovskite FE structure. Patterns and shifting in the patterns due to changes in temperature explore the phase transition behavior by XRD, FTIR analysis, dielectric and ferroelectric studies [15]. These investigations suggest this way of changing the structural phase, size of the particles, absorption patterns, and conduction mechanism in ferroelectrics.

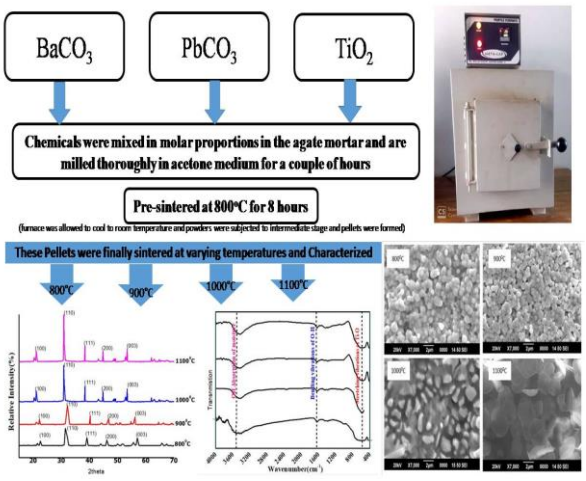

Fig. 1 – Schematic aim of the present paper

The main objective of the work is to synthesize barium doped lead titanate ($Ba_{0.15}Pb_{0.85}TiO_3$) by the low-cost solid-state method with different sintering temperatures. Obtained structural, morphological, FTIR and mechan-

* physicssiddu@gmail.com

ical properties of ferroelectrics are elaborately reported. The W-H plot and size-strain plots were studied in a widespread way and the results have been compared.

2. EXPERIMENTAL PROCEDURE

The barium doped lead titanate was prepared by the solid-state reaction or ceramic method. In this method, high purity divalent metal oxide and FE oxide were mixed thoroughly with the required molar proportion in wet medium acetone. The mixture was then pre-sintered at an elevated temperature for several hours to form a FE powder. This powder was dried and pressed into a suitable shape and finally sintered at a high temperature of about 800 °C to 1100 °C for a few hours. In sintering processes, the transfer of heat energy to a compressed and compact densified pellet leads to a change in grain size, as well as to the purity of ceramic material and to the maintenance of uniformity of materials. Ferroelectrics with general formula $Ba_xPb_{1-x}TiO_3$ ($x = 0.15$) were prepared by ceramic method using AR grade $PbCO_3$, $BaCO_3$ and TiO_2. These chemicals were mixed in molar proportions in the agate mortar and milled thoroughly in acetone medium for 4 h. These mixed powders were pre-sintered at 800 °C for 8 h and the furnace was allowed to cool to room temperature. Powders were subjected to intermediate stage and pellets were formed using hydraulic press by applying a pressure of samples about seven tons per five min. Further, pellets were finally sintered at varying temperatures of about 800 °C, 900 °C, 1000 °C and 1100 °C for 10 h in air medium.

3. RESULTS AND DISCUSSION

3.1 XRD Analysis

The diffraction pattern is presented to give diffraction peaks, which can be attributed to tetragonal [16] perovskite structure and which are tabulated values with the help of the JCPDS data. The observed peaks confirm that a single pure phase is formed. The estimated lattice parameters a and c for the prominent peak (110) are in good agreement with earlier reports. For the tetragonal structure, the interplanar spacing d, the lattice parameters a and c and Miller indices (hkl) are related by

$$\frac{1}{d^2} = \frac{h^2 + k^2}{a^2} + \frac{l^2}{c^2} \qquad (1)$$

Hence lattice parameters a and c can be found. The crystallite size D is calculated from the full width half maximum (FWHM) of XRD peaks at 2θ using the Scherrer formula

$$D = \frac{K \cdot \lambda}{\beta_D . \cos\theta}, \qquad (2)$$

where K is the Scherrer constant ($K = 0.9$), θ is the Bragg angle, and β is FWHM in radians. The results for cell parameters, crystallite size D, and cell volume V are collected in Table 2.

The values of particle sizes and microstrain of the samples are given in Table 1. The particle sizes were found to be varying from 21.11 to 24.35 nm. Microstrain at 900 °C is relatively lower (1.488×10^{-3}) than that at 1100 °C (1.834×10^{-3}). Influence of sintering temperature was also observed in microstrain. Because of different factors such as lattice defects, presence of impurities, large surface energy and thermal history and many more [18, 19] the strain may increase. Where the samples show almost identical particle sizes, this is due to the same rate of ferrites formation for the same compositions favoring the same particle sizes.

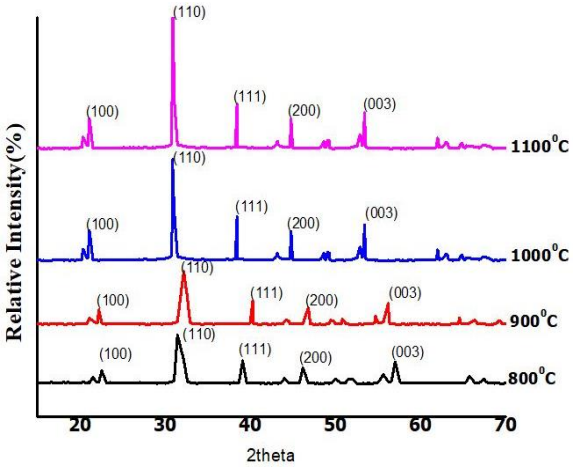

Fig. 2 – XRD patterns of barium doped lead titanate

Table 1 – Data on particle size, dislocation density and microstrain

Sample (°C)	Particle size (nm)	Dislocation density (m^2)(10^{15})	Microstrain ($\times 10^{-3}$)
800	24.21	1.80	1.489
900	24.35	1.83	1.488
1000	24.21	1.81	1.489
1100	21.11	2.88	1.834

Table 2 – Lattice parameters, cell volume V, and crystallite size

Sample (°C)	Lattice parameters, Å		V, Å^3	D, nm
	a	c		
800	3.987	4.068	64.67	24.21
900	3.942	4.134	64.26	24.35
1000	3.912	4.221	64.59	24.21
1100	3.949	4.220	63.09	21.11

3.2 FTIR Analysis

The absorption bands around 575 cm^{-1} to 585 cm^{-1} are assigned to the stretching vibrations of Ti–O bonds. The sharp absorption peaks observed around 3400 to 3450 cm^{-1} indicate that the presence of OH–groups is due to absorption of moisture or vapor from the atmosphere, whereas the peaks around 1400 to 1600 cm^{-1} are attributed to O–H bending vibrations. The absorption bands around 1000 to 1050 cm^{-1} are assigned to the coupling or stretching mode between Ti–O bonds. The shifting of peaks in the range 575 to 585 cm^{-1} towards higher wavenumbers with a decrease in temperature is attributed to the enhancement of the Ti–O bond length; and shifting of the peak towards lower wavenumbers with an increase in temperature is due to distortion of the Ti–O bond length.

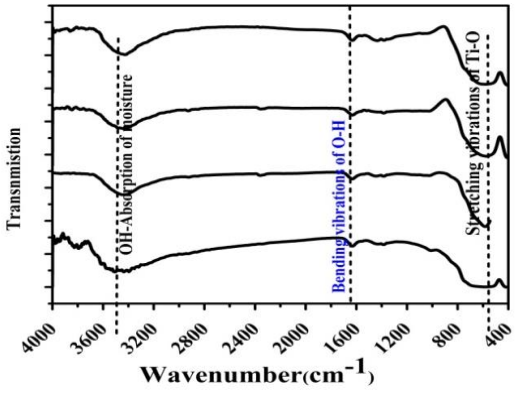

Fig. 3 – FTIR spectra of $Ba_xPb_{1-x}TiO_3$

Table 3 – Dislocation density ρ_D and microstrain ε for PBT sample

Sintering temperature (°C)	$\rho_D \times 10^{15}$ (m^2)	$E \times 10^{-3}$
800	1.81	1.489
900	1.83	1.488
1000	1.81	1.489
1100	2.88	1.834

3.3 Mechanical Properties, W-H Plot and SSP Plots

Crystallographic defects are interruptions of regularly arranged patterns in crystalline solids. Every interruption is common because the positions of atoms at repeated prefixed distances determine the unit cell parameters in crystals, in which a crystalline solid is periodically formed and it is usually imperfect. The number of defects in crystals is evaluated in terms of dislocation density in the system. The dislocation density (ρ_D) is the number of dislocations per unit volume in crystalline materials. Decrease in the dislocation density and increase in the grain size, which are the more perfect crystallization processes, can be seen at 800 °C and 1000 °C. The term lattice microstrain (ε) is used frequently in materials engineering. It is defined as the deformation of an object divided by its effective length. The dislocation density ρ_D and microstrain ε were calculated as

$$(\rho_D) = \frac{1}{D^2}, \tag{3}$$

$$micro-strain(\varepsilon) = \frac{\beta \cos\theta}{4} \tag{4}$$

with their results listed in Table 3, and the values of ε can be calculated using the Williamson-Hall plot

$$\frac{\beta\cos\theta}{\lambda} = \frac{\varepsilon \sin\theta}{\lambda} + 1/D, \tag{5}$$

where λ is the wavelength of X-rays used (1.542 Å).

Eq. (5) is in the format $Y = mx + n$, where $m = \varepsilon/\lambda$ and $n = 1/D$. By plotting $\beta\cos\theta$ as a function of $\sin\theta$, we can find ε from the slope and $1/D$ as an intercept. Fig. 4 illustrates the Williamson-Hall plots of $\beta\cos\theta$ vs. $\sin\theta$ for PBT samples.

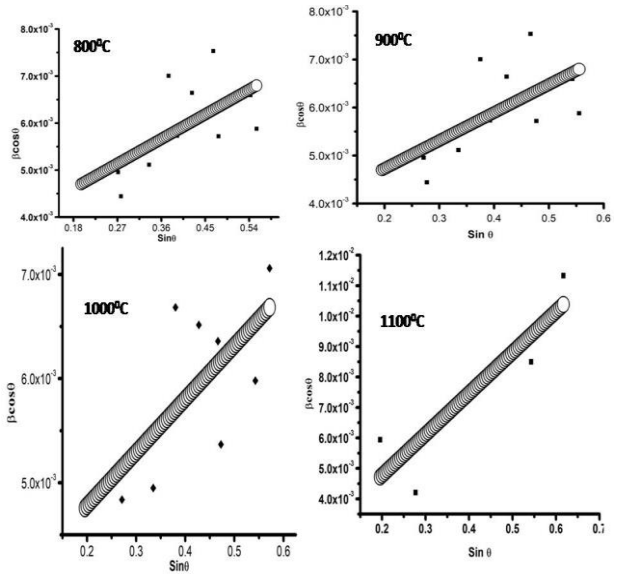

Fig. 4 – Williamson-Hall plots of $\beta\cos\theta$ vs. $\sin\theta$ for PBT

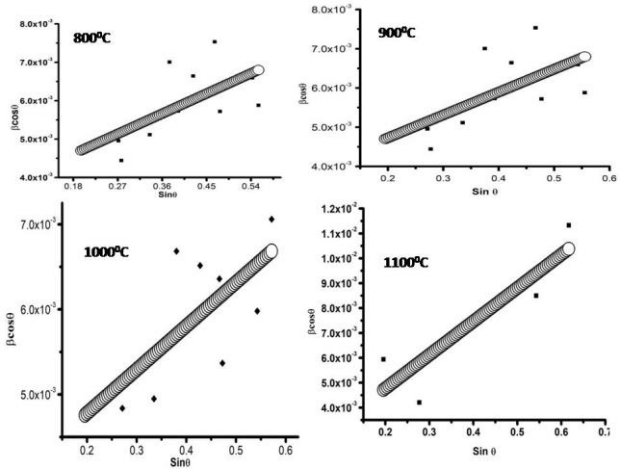

Fig 5 – SSP plots of PBT samples

The evaluation of the size-strain parameters (SSP) is obtained by considering peaks in an average range, which has the advantage that less weight is given to the data from reflections at high angles, where the precision is usually less. The SSP plots are shown in Fig. 5 which are plotted using Eq. (5). In this approximation, SSP plots assume that the "crystallite size profile" is Lorentzian and the "strain profile" is a Gaussian function [20, 21]. Accordingly, we have:

$$(d_{hkl}\beta_{hkl}\cos\theta)^2 = \frac{K\lambda}{D}(d_{hkl}^2\beta_{hkl}\cos\theta) + \left(\frac{\varepsilon}{2}\right)^2. \tag{5}$$

The correlation between W-H and SSP plots is given in Table 4.

Sample (°C)	W-H plot		SS plot	
	Crystallite size D (nm)	Strain (ε)	Crystallite size D (Å)	Strain (ε)
800	51	0.005	117	0.055
900	43	0.0058	117	0.055
1000	50	0.005	119	0.054
1100	75	0.013	88	0.0721

Table 5 – Texture coefficients (TC) for significant (*hkl*) planes of PBT samples

Plane			TC (*hkl*)			
h	*k*	*l*	800 °C	900 °C	1000 °C	1100 °C
1	0	0	1.3159	1.4099	1.3159	1.3159
1	0	1	0.0272	1.1833	0.0272	0.0272
1	1	0	2.4208	1.2149	2.4208	2.4208
1	1	1	1.4728	1.3988	1.4728	1.4728
0	0	2	0.1375	0.6722	0.1375	–
2	0	0	0.0887	1.2430	0.0887	0.1375
0	1	2	0.3488	–	0.3488	–
1	1	2	1.3028	1.7323	1.3028	–
2	1	1	0.1543	1.1386	0.1543	–
2	1	2	1.8814	–	1.8814	–
0	0	3	1.7329	–	–	–
2	2	0	–	1.2980	–	–
2	0	2	1.1171	–	1.1171	0.0887
0	0	3	–	0.9662	1.7329	–

3.4 Texture Analysis

The reflection intensities of the XRD patterns contain information about the growth of polycrystalline materials and also random orientation which has predictable peak intensity, which is studied by calculating texture coefficients TC (*hkl*) for all the planes by using formula defined as

$$TC(hkl) = \frac{\frac{I(hkl)}{I_0(hkl)}}{\frac{1}{N}\sum_N \frac{I(hkl)}{I_0(hkl)}}, \qquad (6)$$

where $I(hkl)$ is the measured intensity of reflection, $I_0(hkl)$ corresponds to the standard intensity from the JCPDS Card, N is the number of reflections observed in the XRD patterns.

The reflections in the XRD patterns explain phase growth in a polycrystalline PBT structure. All the PBT structures show strong orientation about (110) plane compared to other planes but the orientation varies from 2.42081 to 1.33062. Similar results were observed for dislocation density. If TC (*hkl*) value > 1 then (*hkl*) planes under considerations are randomly oriented crystallites, but if TC (*hkl*) < 1 this indicates the abundance of grains in the given (*hkl*) direction. For different sintering temperatures 800, 900, 1000 and 1100 °C, grain orientation less than 1 indicates the lack of orientation. As the TC (*hkl*) increases, the growing crystallites in the directions perpendicular to the (*hkl*) plane becomes maximally pronounced and randomly oriented crystallites in the direction larger than TC (*hkl*) values that is the result of available abundance of crystallites oriented in the (*hkl*) direction. The arrangement of the crystals grains decides the use in different applications which metals, ceramics polycrystalline texture which deals with the properties and that helps to decide applications.

Fig. 6 shows the SEM micrographs of Pb-Ba-TiO_3 samples sintered at 800, 900, 1000 and 1100 °C for a few hours, and these images show the development of the grain morphology and dense microstructure.

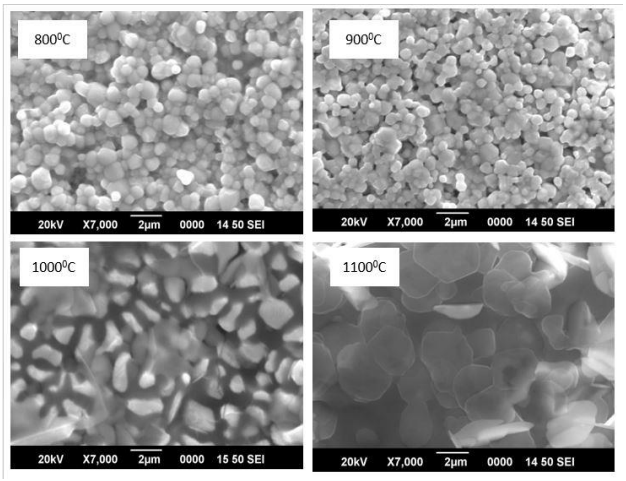

Fig. 6 – SEM images of PBT

3.5 SEM Analysis

The calculated grain size is shown in Table 4, but at temperatures ranging from 800 °C to 1100 °C it varies from 0.6375 μm to 1.713 μm; these results may show that segregation of impurity phases is not observed. The increase in grain diameter is attributed to the diffusion of barium, oxygen vacancies and pores without deposition on grain boundaries which hamper the grain growth. The decrease in grain diameter is attributed to smaller solubility of Ba. The exaggerated grain growth occurs on account of lack of chemical homogeneity, variation in density and presence of impurities [22].

4. CONCLUSIONS

Lead-Barium-Titanate (PBT) powder has been successfully synthesized by a cost-effective ceramic method or solid-state reaction method. PBT characterization has been done with XRD data which reveals the information on the formation of a tetragonal perovskite structure for $Pb_{1-x}Ba_xTiO_3$ (sintering temperatures 800, 900, 1000 and 1100 °C). The unit cell parameters a and c were found to vary from 3.98 to 4.068. The dislocation density of samples lies in the range of $(1.88\text{-}2.88) \times 10^{-15}$. To our knowledge, texture analysis, dislocation density and mechanical properties of $Pb_{1-x}Ba_xTiO_3$ have been reported for the first time.

ACKNOWLEDGEMENTS

The SNM wishes thanks to Prof. Gloria Albert, Department of English, KLEIT, Hubballi, India for proofreading the article.

REFERENCES

1. Y. Xu, *Ferroelectric Materials and Their Applications* (New York: Elsevier Science Publishers: 1991).
2. A.P. Kuzmenko, I.V. Chuhaeva, P.V. Abakumov, M.B. Dobromyslov, *J. Nano- Electron. Phys.* **8** No 4, 04043 (2016).
3. S.N. Fedosov, H. von Seggern, *J. Nano.- Electron. Phys.* **5** No 4, 04056 (2013).
4. D.A. Kovalenko, V.V. Petrov, *J. Nano- Electron. Phys.* **7** No 3, 03036 (2015).
5. D.A. Kiselev, S.A. Levashov, M.S. Afanasiev, A.M. Kiselev, G.V. Chucheva, *J. Nano- Electron. Phys.* **8** No 3, 03027 (2016).
6. S. Chamaani, S.A. Mirtaheri, M. Teshnehlab, M.A. Shoorehdeli, V. Seydi, *Prog. Electromag. Res.* **79**, 353 (2008).
7. F. Li, D. Lin, Z. Chen, *Nature Mater.* **17**, 349 (2018).
8. S.N. Mathad, M.K. Rendale, R.N. Jadhav, V. Puri, *Proc. Appl. Ceram.* **10**, 41 (2016).
9. S.N. Mathad, R.N. Jadhav, R.P. Pawar, V. Puri, *Adv. Sci. Eng. Med.* **5**, 789 (2013).
10. S.N. Mathad, R.N. Jadhav, V. Phadtare, V. Puri, *Int. J. Self-Propag. High Temp. Synthes.* **23**, 145 (2014).
11. R. Jacob, J. Isac, *Int. J. Sci. Res. Publ.* **4** No 12, 2250 (2014).
12. K. Konstantinov, S.H. Ng, J.Z. Wang, G.X. Wang, D. Wexler, H.K. Liu, *J. Power Source.* **159** No 1, 241 (2006).
13. A. Thulasiromudu, S. Buddhudu, *Spectrachim. Acta. A* **66** No 2, 323 (2007).
14. C. Barriga, S. Maffi, L.P. Bicelli, C. Malitesta, *J. Power Source.* **34**, 353 (1991).
15. A. Dixit, S.B. Majumder, P.S. Dobal, R.S. Katiyar, A.S. Bhalla, *Thin Solid Films* **447**, 284 (2004).
16. K.K. Patankar, V.L. Mathe, R.N. Patil, B.K. Chougule, *Mat. Chem. Phys.* **96**, 197 (2006).
17. S.D. Likhite, C. Radhakrihnamurthy, P.W. Sahastrabudhe, *Rev. Sci. Inst.* **25**, 302 (1965).
18. J. Jankovskis, V. Yurshevich, V. Scavinskis, *Electrotechnika* **5**, (2005).
19. M. Schaefer, C.A. Grant, E.C. Sklute, *Ann. Rev. Earth Planet. Sci.* **34**, 83 (2006).
20. Y.T. Prabhu, K.V. Rao, V.S.S. Kumar, B.S. Kumari, *World J. Nano Sci. Eng.* **4**, 21 (2014).
21. H.R. Shashidhargouda, N. Mathad, *Ovidius University Ann. Chem.* **29** No 2, 122 (2018).
22. Dazhi Sun, Xueqing Jin, Heng Liu, Jie Zhu, Yudan Zhu, Yinyin Zhu, *Ferroelectrics* **355** No 1, 145 (2007).

Структурно-механічні дослідження сегнетоелектриків $Ba_xPb_{1-x}TiO_3$ в залежності від температури спікання

Sadiya Kazi[1], Feeda Savanur[1], Sushant Kakati[2], Shridhar N. Mathad[2], P.R. Jeergal[1], A.S. Pujar[3], C.S. Hiremath[4], S.L. Galgali[3], M.K. Rendale[5], R.B. Pujar[1]

[1] *Departmant of Physics, P.C. Jabin Science College, Hubballi, India*
[2] *Department of Engineering Physics, K.L.E. Institute of Technology, Gokul Road, Hubballi, 580027 Karnataka, India*
[3] *Department of Physics, KLE's RLS Institute, Belgavi, India*
[4] *Department of Physics, H.S.* Kotambri *Science Institute, Hubballi, India*
[5] *Department of Physics, Gogte Institute of Technology, Belgavi, India*

Сегнетоелектрична кераміка свинцю-барію-титанату (PBT) синтезувалась за допомогою методу твердотільної реакції з різними температурами спікання. Структура зразків характеризувалася рентгенівською дифракцією (XRD), скануючою електронною мікроскопією (SEM) та інфрачервоною спектроскопією з перетворенням Фур'є (FTIR). XRD зразків Pb-Ba-TiO_3 підтверджує тетрагональну перовскітну сегнетоелектричну структуру з параметрами решітки в діапазоні 3,94-3,987 Å і 4,068-4,22 Å. Зростання зерен збільшується з температурою спікання, і за допомогою SEM аналізу розмір зерна досліджуваних зразків виявляється в межах 0,6-1,713 мкм. З аналізу FTIR випливає, що смуги поглинання близько 575 $см^{-1}$-585 $см^{-1}$ відносяться до коливань розтягування зв'язків Ti–O. Повідомляється також про розмір кристалітів (D), постійну решітки (a), мікронапруження (ε) та густину дислокацій (ρ_D). Графік Вільямсона-Холла та залежність розміру зерна від напружень також використовуються для розуміння структурних та механічних ознак сегнетоелектричних зразків. Таким чином, ми повідомляємо про зміну структурно-механічних властивостей PBT залежно від температури спікання.

Ключові слова: Рентгенівська дифракція, Сегнетоелектрики, Морфологія.